

## USING SPHERICAL SHELLS FOR GAIN ENHANCEMENT OF COMPACT WIDEBAND PHASED ARRAYS

Abdelnasser A. Eldek\*

Department of Computer Engineering, Jackson State University, Jackson, MS 39217, USA

**Abstract**—Spherical shells are proposed and presented to improve the gain of a class of wideband phased array systems. This kind of phased arrays is composed of compact elements, which allow for a small distance between elements that is much less than half wavelength at lower operating frequencies. This small distance, as a function of wavelength, results in a small gain. Therefore, shells confronting the array are proposed to improve the gain. The formulations required to define the geometry and material properties of the shell are developed. Two and four element arrays are designed and simulated with and without shells to test the technique, and promising results are obtained at lower frequencies for the array with shells.

### 1. INTRODUCTION

Modern wireless communication systems often require wideband performance for multi-function and multi-channel operations. One of the most important components of these systems is phased array antenna because of its ability to steer the beam very fast by an appropriate inter-element phase control [1]. Ideally, phased array antenna system needs to be wideband with large scanning angle. Such system has to be composed of wideband radiation elements with stable radiation patterns of acceptable gain, low cross polarization, and high front-to-back ratio. The maximum steering angle is within the 3 dB beamwidth of the antenna co-polarized pattern; therefore wide 3 dB beamwidth is an important characteristic of the array element. Researchers have done a lot of effort to design wideband elements with stable patterns and wide 3 dB beamwidth for phased arrays [2–7].

---

*Received 4 March 2013, Accepted 8 April 2013, Scheduled 10 April 2013*

\* Corresponding author: Abdelnasser A. Eldek (abdelnasser.eldek@jsums.edu).

These efforts concentrated on increasing the antenna impedance bandwidth and enhancing its patterns and pattern stability. However, when using these antennas in phased arrays, many challenges arise. If the distance between elements is more than half wavelength (at higher operating frequencies), grating lobes appear, which limit the array scanning capability and make the usable bandwidth of the phased array much less than the bandwidth of the antenna. For example, the bandwidth of the antenna presented in [5] is more than 100%, while the usable bandwidth of the array is 71%. On the other hand, if the adjacent elements, sharing the same substrate, are too close, this increases the coupling due to the traveling waves in the substrate. High coupling may cause scan blindness and anomalies within the desired bandwidth and scan volume [8, 9]. In addition, the small distance with respect to wavelength (at low operating frequencies) results in low gain.

To overcome this problem, some researchers used pattern synthesis. They introduced intentional nulls on the element pattern at the locations of the grating lobes to be nullified [10]. In [11, 12], single asymmetric ridge waveguide was used for linear arrays to achieve close element spacing in the scan plane and avoid grating lobes. These two techniques were applied on narrowband arrays like slotted waveguide and patch antenna arrays. A wideband linear phased array with unequal space was introduced in [13]. The patterns were synthesized so that no grating lobes would arise in wideband. Genetic algorithms were used for sub-array amplitude weighting to reduce grating lobes, and presented in [14] for limited scanning only. A tapered balun was designed and introduced for broadband array with closely spaced elements [15]. This design was complex because the radiating elements and the tapered balun were perpendicular to each other.

In this effort, the double rhombus antenna presented in [5] is modified to reduce the size. Then, this miniaturized antenna is used to compose a compact wideband phased array with small element spacing. When the distance between elements decreases, the gain decreases significantly because this distance becomes close to quarter wavelength. Therefore, there is a need for gain improvement technique at these frequencies, which is presented also in this paper. Spherical shells are proposed to improve the gain of this array at low operating frequencies. The results shown in this paper are obtained from Ansoft High Frequency Structure Simulator (HFSS), which is based on Finite Element [16].

## 2. COMPACT WIDEBAND ANTENNA DESIGN

First, the double rhombus antenna [5] is modified to reduce its size. The antenna is printed on a Rogers RT/Duroid 6010 LM substrate of 10.2 dielectric constant, 0.0023 conductor loss ( $\tan \delta$ ), and 25 mil (0.635 mm) thickness. The width of the original antenna is 12 mm, and the smallest distance between elements (center to center) is 14 mm. In this case, grating lobes start after 10.7 GHz. Therefore, the largest element in this antenna, which is the longer branch, is modified and studied (see Fig. 1). Then, this branch is fixed to 8.5 mm. After that, all other parameters are tuned using parametric study to obtain wide bandwidth, and to decrease the lower operating frequency. The antenna parameters and dimensions are illustrated in Fig. 1 and Table 1, respectively. The return loss of this design is shown in Fig. 2. The antenna is operating from 6.5 GHz to 16.2 GHz with a total bandwidth of 86%. The antenna width (8.5 mm) is 30% less than the one in [5]. In terms of wavelength, the antenna width is  $0.18\lambda_L$  and  $0.44\lambda_H$ , while the original one was  $0.22\lambda_L$  and  $0.72\lambda_H$ . The small size of the new design allows for a smaller distance between elements ( $d = 11$  mm instead of 14 mm). This distance is  $0.59\lambda$  at

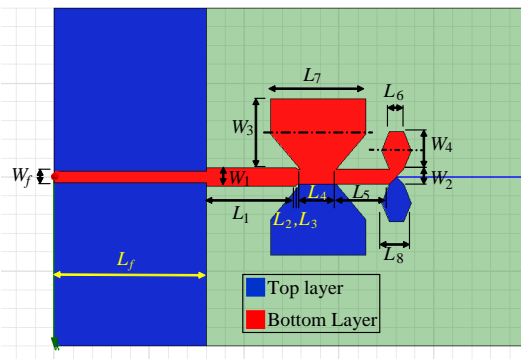


**Figure 1.** The miniaturized antenna with 8.5 mm width.

**Table 1.** Dimensions in mm for the antenna in Fig. 1.

$W_f$	$W_1$	$W_2$	$W_3$	$W_4$	$L_f$	$L_1$
0.6	1.0	0.6	3.75	2	8	4.7
$L_2$	$L_3$	$L_4$	$L_5$	$L_6$	$L_7$	$L_8$
0.2	0.15	1.9	2.8	0.75	5	1.55

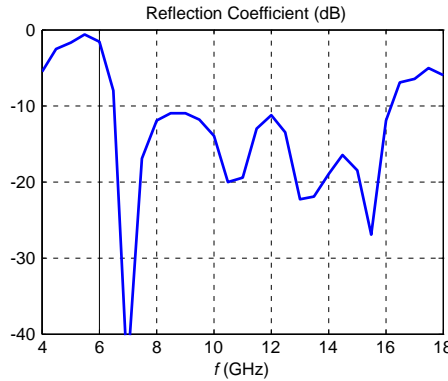


**Figure 2.** Return loss for the antenna in Fig. 1.

16.2 GHz, which makes grating lobes insignificant for this array at all frequencies. However, since this distance is around quarter wavelength at 6.5 GHz, low gain is expected. Therefore, in the next section, spherical shells confronting the array are proposed to increase the gain at lower frequencies, to the same value when “ $d$ ” is half wavelength, which is the case with the best gain without grating lobes.

### 3. SHELL DESIGN FORMULATIONS

For a point source array in  $z$  direction, the array factor (AF) is defined as:

$$AF = [\sin(N\psi/2)]/(N/2), \quad (1)$$

where  $\psi = 2\pi D \cos \theta + B$  and  $D = d/\lambda$ . The best results (maximum directivity without grating lobes) are obtained when  $D = 0.5$  (call it Array 1). In this case,  $\psi_1 = \pi \cos \theta + B$ . Assume that we have a second array (Array 2) with  $D = 0.5q$ , then,  $\psi_2 = q\pi \cos \theta + B_2$ . Fig. 3 shows and compares the AF of Array 2, when  $N = 8$  and  $q = 0.5$ , with that of the ideal one ( $q = 1$ ). A clear reduction in the directivity in Array 2 is noticed at  $\theta_0 = 90^\circ$  and  $45^\circ$ . In addition, this affects the maximum steering angle, as the directivity decreases when the steering angle increases (see Fig. 3 at  $45^\circ$ ).

To improve the radiation patterns when  $q = 0.5$ ,  $\psi_2$  is required to be equal to  $\psi_1$ . Then

$$q\pi \cos \theta + B_2 = \pi \cos \theta + B, \quad \text{or} \quad B_2 = B + (1 - q)\pi \cos \theta, \quad (2)$$

where  $B$  is the phase shift required for beam steering in the ideal array. Assume that  $q = 0.5$  again, and assume that we are able to add the

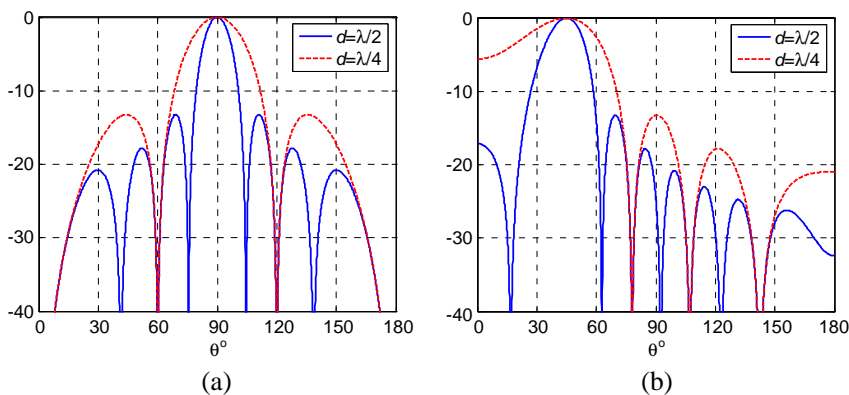


**Figure 3.** Array factor for  $d = 0.25\lambda$  and  $0.5\lambda$ , at (a)  $\theta_0 = 90^\circ$  and (b)  $45^\circ$ .

phase shift  $B_2$  as in (2), then the two array factors of this array and the ideal one will be identical. However, the problem is how to add a delay which is a function of  $\theta$ . Fig. 4(a) shows  $(B_2 - B)$  vs.  $\theta$ .  $(B_2 - B)$  is  $\pi/2$  at  $\theta = 0^\circ$ , 0 at  $90^\circ$  (direction of the maximum radiation for the proposed array), and  $-\pi/2$  at  $\theta = 180^\circ$ . From  $0^\circ$  to  $90^\circ$ , it is required to gradually delay radiation by certain time which decreases to 0 at  $90^\circ$ . This can be done by adding delaying materials facing the array at these angles. Between  $90^\circ$  and  $180^\circ$ , we need to speed up the radiation by adding a material in which the electromagnetic waves travel in a speed more than the speed of light, which is practically impossible right now. To solve this problem let us shift the whole curve in Fig. 4(a) up by  $\pi/2$ . Then,

$$B_2 = B + \frac{\pi}{2} \cos \theta = \left[ B - \frac{\pi}{2} \right] + \left[ \frac{\pi}{2} \cos \theta + \frac{\pi}{2} \right] = B_c + B_v. \quad (3)$$

The first term,  $B_c$ , is constant for all array elements. The second term,  $B_v$ , is variable and it is a function of  $\theta$ , as shown in Fig. 4(b).

One suggestion to add this delay is to add a material with both permittivity and permeability in the front of the antenna as shown in Fig. 5, where the thickness  $r$  is proportional with  $B_v$ , and can be approximated as follow:

$$r = [\cos \theta + 1] R_0/2, \quad (4)$$

where  $R_0$  is the maximum value of  $r$ . The maximum delay ( $\pi$ ) happens at  $\theta = 0^\circ$ , where  $r = R_0$ . This delay can be calculated by comparing the electromagnetic wave travel time inside the dielectric with its travel

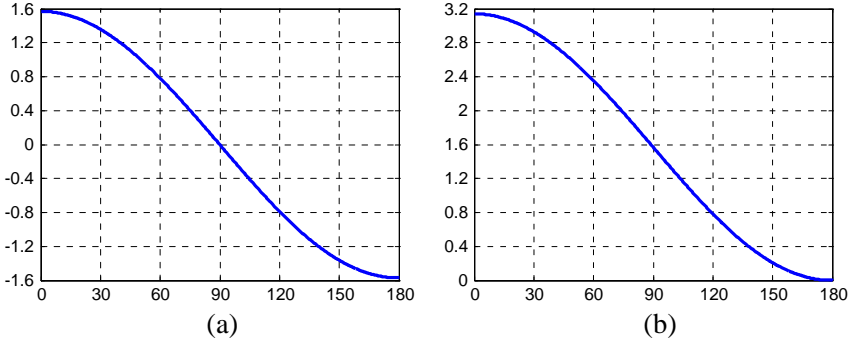


**Figure 4.** (a)  $(B_2 - B)$  vs.  $\theta$  when  $q = 0.5$  and (b) shifted by  $\pi/2$ .

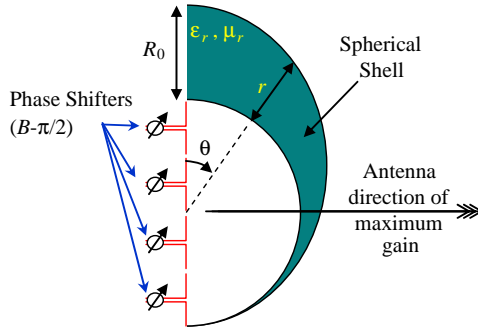


**Figure 5.** Spherical shell geometry confronting a 4-element array.

time in free space (without shell). Then,

$$Delay_{\max} = \omega t_{\max} = \omega \left[ \frac{R_0}{c} \sqrt{\mu_r \epsilon_r} - \frac{R_0}{c} \right] = \pi, \quad (5)$$

where  $c$  is the speed of light,  $\omega = 2\pi f$ , and  $f$  is the frequency. Then  $R_0$  can be calculated from (5) as follow:

$$R_0 = \frac{c}{2f (\sqrt{\mu_r \epsilon_r} - 1)}. \quad (6)$$

Substitute by  $R_0$  in (4), then

$$r = \frac{[\cos \theta + 1]}{2} \cdot \frac{c}{2f (\sqrt{\mu_r \epsilon_r} - 1)} = \frac{c (\cos \theta + 1)}{4f (\sqrt{\mu_r \epsilon_r} - 1)}. \quad (7)$$

Based on this formula, the required dielectric shell will be similar to the one shown in Fig. 5.

#### 4. RESULTS

In order to verify the validity of these formulations and technique, two arrays are designed: 2-element and 4-element arrays. Fig. 6 shows the geometries of these arrays with shells. The gains of the regular arrays are calculated using Ansoft HFSS then compared with the gains with shells at 7 and 9 GHz (low operating frequencies). It is expected that gain will be enhanced more at 7 GHz than at 9 GHz, because the distance between elements at 7 GHz is smaller in terms of wavelength.

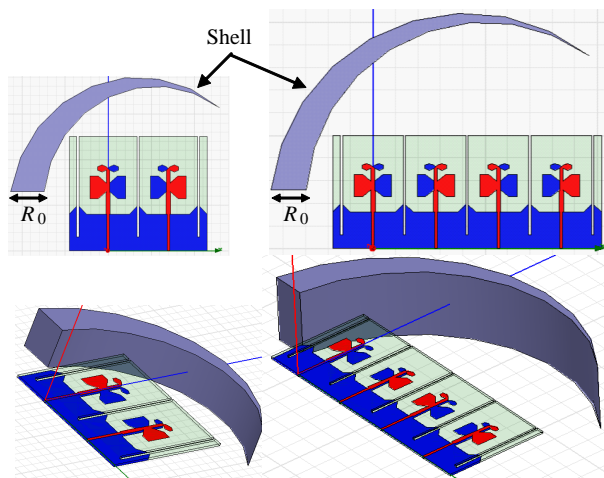


**Figure 6.** 2D and 3D Geometry of 2 and 4-element arrays with dielectric shells.

All the results for 2-element arrays are depicted in Table 2. Without shell, the gain is 4.8 and 7.81 dB at 7 and 9 GHz, respectively. Then, different shell is added for each frequency. The inner and outer radii of the shell are 26 and 30 mm, respectively, and its height is 10 mm plus the substrate height. The shell height is then increased to 20 mm to study its effect on the gain (see Table 2). At 7 GHz, the shell improves the gain from 4.8 to 7.37 dB (53.5% increase). At 9 GHz, the improvement in the gain is not remarkable when  $\epsilon_r = \mu_r = 3.15$  as calculated from (7). Therefore, other materials are studied with different  $\epsilon_r$  and  $\mu_r$  values. The gain is found to be improved more when  $\epsilon_r$  and  $\mu_r$  decrease with a maximum gain at  $\epsilon_r = \mu_r = 2.2$ . The gain improvement is 7.4%. When the shell height is increased to 20 mm, the gain improvement becomes better (55% and 11% at 7 and 9 GHz compared to 53.5% and 7.4%).

The same results are repeated for 4-element arrays, and the results

**Table 2.** Maximum gain for 2-element arrays with and without shells and the percentage increment when adding shells of two different heights: 10 and 20 mm.

	7 GHz		9 GHz	
<b>Array without Shell</b> →	4.80		7.81	
<b>Shell:</b> $\varepsilon_r = \mu_r = 4$ (10 mm height)	7.37	53.5%		
<b>Shell:</b> $\varepsilon_r = \mu_r = 4$ (20 mm height)	7.44	55.0%		
<b>Shell:</b> $\varepsilon_r = \mu_r = 3.15$ , (10 mm height)			7.87	0.8%
<b>Shell:</b> $\varepsilon_r = \mu_r = 2.8$ , (10 mm height)			8.16	4.5%
<b>Shell:</b> $\varepsilon_r = \mu_r = 2.4$ , (10 mm height)			8.37	7.2%
<b>Shell:</b> $\varepsilon_r = \mu_r = 2.2$ , (10 mm height)			8.39	7.4%
<b>Shell:</b> $\varepsilon_r = \mu_r = 2.2$ , (20 mm height)			8.67	11.0%

**Table 3.** Maximum gain for 4-element arrays with and without shells and the percentage increment when adding shells of two different heights: 10 and 20 mm.

	7 GHz		9 GHz	
<b>Array without Shell</b> →	6.81		10.46	
<b>Shell:</b> $\varepsilon_r = \mu_r = 4$ (10 mm height)	8.39	23.2%		
<b>Shell:</b> $\varepsilon_r = \mu_r = 4$ (20 mm height)	8.52	25.1%		
<b>Shell:</b> $\varepsilon_r = \mu_r = 2.2$ , (10 mm height)			11.23	7.4%
<b>Shell:</b> $\varepsilon_r = \mu_r = 2.2$ , (20 mm height)			11.42	9.2%

are summarized in Table 3. At 7 GHz, the shell improves the gain from 6.81 to 8.39 dB (23.2% increase). At 9 GHz, the improvement in the gain is 7.4% when  $\varepsilon_r = \mu_r = 2.2$ . When the shell height is increased to 20 mm, the gain improvement becomes 25.1% and 9.2% at 7 and 9 GHz. These results show that the shell is effective at low frequencies.

## 5. CONCLUSIONS

The double rhombus antenna is modified, and the new design is 30% less in size with 86% bandwidth. Formulations are developed and presented for designing spherical shell to enhance the gain of an array with these small antennas, where the distance between elements is much smaller than half wavelength. Two and four element arrays are designed with and without shells to test the technique. Good enhancement in the gain is obtained especially at 7 GHz, where the distance between elements is close to quarter wavelength.



## ACKNOWLEDGMENT

The author would like thank the Air Force Research Laboratory (AFRL) — Minority Leaders Program (MLP), and Clarkson Aerospace Corp for funding this research through contract number FA8650-05-D-1912.

## REFERENCES

1. Parker, D. and D. C. Zimmermann, "Phased Arrays — Part I: Theory and architectures," *IEEE Trans. Antennas Propagat.*, Vol. 50, No. 3, 678–687, Mar. 2002.
2. Eldek, A. A., "Pattern stability optimization for wideband microstrip antennas for phased arrays and power combiners," *Microwave Opt. Tech. Lett.*, Vol. 48, No. 8, 1492–1494, Aug. 2006.
3. Eldek, A. A., "Design of double dipole antenna with enhanced usable bandwidth for wideband phased array applications," *Progress In Electromagnetics Research*, Vol. 59, 1–15, 2006.
4. Eldek, A. A. and G. Zheng, "A microstrip-fed quasi-rhombus shape double dipole antenna for wideband phased array applications," *Microwave Opt. Tech. Lett.*, Vol. 48, No. 12, 2461–2464, Dec. 2006.
5. Eldek, A. A., "Ultra wideband double rhombus antenna with stable radiation patterns for phased array applications," *IEEE Trans. Antennas Propagat.*, Vol. 55, No. 1, 84–91, Jan. 2007.
6. Eldek, A. A., "Wideband 180 degree phase shifter using microstrip-CPW-microstrip transition," *Progress In Electromagnetics Research B*, Vol. 2, 177–187, 2008.
7. Eldek, A. A., "A double rhombus antenna fed by 180 degree phase shifter for ultra wideband phased array applications," *IEEE Trans. Antennas Propagat.*, Vol. 56, No. 6, 1566–1572, Jun. 2008.
8. Chio, T. H. and D. H. Schaubert, "Parameter study and design of wideband widescan dual-polarized tapered slot antenna arrays," *IEEE Trans. Antennas Propagat.*, Vol. 48, 879–886, June 2000.
9. Guo, Y. X., K. M. Luk, and K. F. Lee, "L-probe fed thick-substrate patch antenna mounted on a finite ground plane," *IEEE Trans. Antennas Propagat.*, Vol. 51, 1955–1963, Aug. 2003.
10. Shafai, L., "Scan gain enhancement in phased arrays by element pattern synthesis," *IEE Seventh International Conference on Antennas and Propagation (ICAP 91)*, Vol. 2, 914–917, 1991.
11. Shnitkin, H., J. Green, and P. J. Bertalan, "Asymmetric ridge waveguide radiating element for a scanned planar array," *IEEE*

- Antennas and Propagation Society International Symposium*, Vol. 1, 55–58, 1988.
12. Green, J., H. Shnitkin, and P. J. Bertalan, “Asymmetric ridge waveguide radiating element for a scanned planar array,” *IEEE Trans. Antennas Propagat.*, Vol. 38, No. 8, 1161–1165, 1990.
  13. Song, C. and Q. Wu, “A wide-band phased array antennas with unequal space,” *5th Global Symposium on Millimeter Waves (GSMM)*, 393–396, May 2012.
  14. Wang, H., D.-G. Fang, and Y. L. Chow, “Grating lobe reduction in a phased array of limited scanning,” *IEEE Trans. Antennas Propagat.*, Vol. 56, No. 6, 1581–1586, 2008.
  15. Xia, T., S. Yang, and Z. Nie, “Design of a tapered balun for broadband arrays with closely spaced elements,” *IEEE Antennas and Wireless Propagation Letters*, Vol. 8, 1291–1294, 2009.
  16. Ansoft Corporation, “HFSS: high frequency structure simulator based on the finite element method,” Version 14, Ansoft Corp., Canonsburg, PA, 2012.